Packet Structure and Receiver Design for Low Latency Wireless Communications With Ultra-Short Packets

Byungju Lee[©], *Member, IEEE*, Sunho Park[©], *Member, IEEE*, David J. Love[©], *Fellow, IEEE*, Hyoungju Ji, *Member, IEEE*, and Byonghyo Shim[©], *Senior Member, IEEE*

Abstract-Fifth generation wireless standards require much lower latency than what current wireless systems can guarantee. The main challenge in fulfilling these requirements is the development of short packet transmission, in contrast to most of the current standards, which use a long data packet structure. Since the available training resources are limited by the packet size, reliable channel and interference covariance estimation with reduced training overhead are crucial to any system using short data packets. In this paper, we propose an efficient receiver that exploits useful information available in the data transmission period to enhance the reliability of the short packet transmission. In the proposed method, the receive filter (i.e., the sample covariance matrix) is estimated using the received samples from the data transmission without using an interference training period. A channel estimation algorithm to use the most reliable data symbols as virtual pilots is employed to improve quality of the channel estimate. Simulation results verify that the proposed receiver algorithms enhance the reception quality of the short packet transmission.

Index Terms—5G wireless communications, short data packets, low latency, Internet of Things, energy harvesting, virtual pilots.

I. INTRODUCTION

FIFTH generation (5G) communication networks will be a key enabler in realizing the Internet of Things (IoT) era and hyper-connected society [2]–[4]. To support real-time applications with stringent delay requirements and massive machine-type devices, communication systems supporting ultra low latency are needed [5]–[7]. For this reason, International telecommunication union (ITU) defined ultra reliable

Manuscript received December 3, 2016; revised May 5, 2017 and August 4, 2017; accepted September 11, 2017. Date of publication September 21, 2017; date of current version February 14, 2018. This work was supported in part by the National Science Foundation (NSF) grant CNS1642982 and the National Research Foundation of Korea (NRF) grant funded by the Korean government (MSIP) (2014R1A5A1011478 and 2016K1A3A1A20006019). This paper was presented at the GLOBECOM, Washington, USA, December 4–8, 2016 [1]. The associate editor coordinating the review of this paper and approving it for publication was A. Tajer. (Corresponding author: Byonghyo Shim.)

- B. Lee and D. J. Love are with the School of Electrical and Computer Engineering, Purdue University, West Lafayette, IN 47907 USA (e-mail: byungjulee@purdue.edu; djlove@purdue.edu).
- S. Park, H. Ji, and B. Shim are with the Institute of New Media and Communications and the School of Electrical and Computer Engineering, Seoul National University, Seoul 08826, South Korea (e-mail: shpark@islab.snu.ac.kr; hyoungjuji@islab.snu.ac.kr; bshim@snu.ac.kr).

Color versions of one or more of the figures in this paper are available online at http://ieeexplore.ieee.org.

Digital Object Identifier 10.1109/TCOMM.2017.2755012

and low latency communication (uRLLC) as one of key use cases for 5G wireless communications.1 One direct way to meet the stringent low latency requirements is to use a shortsized packet. This is in contrast to most current wireless systems whose sole purpose is to transmit long data packets efficiently. Indeed, most current physical layer design relies heavily on long codes to approach Shannon capacity. Sensors and devices in an IoT networks transmit a very small amount of information such as environmental data (e.g., temperature, humidity, and pollution density), locations, and emergency alarm, and thus asymptotic capacity-achieving principles are not relevant to the transmission of short packets. In view of this, 5G physical layer design (e.g., pilot transmission strategy, coding scheme, hybrid automatic repeat request) needs to be reevaluated and potentially redesigned as a whole. Many papers have been dedicated to analyze performance metrics that are relevant to short packet communication, including the maximal achievable rate at finite packet length and finite packet error probability instead of using two classic information-theoretic metrics, the ergodic capacity and the outage capacity [8]–[11]. Finite block-length analysis has been extended to spectrum sharing networks using rate adaptation [12] and wireless energy and information transmission using feedback [13].

In this paper, we consider practical constraints that are encountered when implementing a short packet transmission framework. First, massive and simultaneous communications among autonomous devices will induce inter-device interference at the receiver in an IoT network. In order to control the inter-device interference, a technique to use multiple receive antennas has been proposed by utilizing the spatial degrees of freedom (DoF) provided by multiple receive antennas to balance interference suppression and desired signal power improvement [14]. To implement this approach, the receiver needs to acquire the desired CSI and the interference plus noise covariance. While the desired CSI can be estimated using pilot signals, direct estimation of the interfering CSI is difficult due to the large number of interfering devices in the IoT network. One way to tackle this problem is to use an

¹Three key use cases include enhance mobile broadband (eMBB), massive machine-type communications (mMTC), and ultra reliable and low latency communication (uRLLC) [6].

interference training period in which the interference (plus noise) covariance matrix can be estimated by listening to interference-only transmissions [15]. The main drawback of this approach is that it incurs a severe transmission rate loss since the target transmit device should remain silent during the interference training period. Also, the interference training period would not be large enough in obtaining the reliable estimate of the interference covariance for this short-sized packets, resulting in severe degradation in performance.

Moreover, since current systems are designed to carry long data packets, the pilot transmission period can be made relatively small even though the actual period of pilot signals is large. However, the portion of time used for pilot signals is unduly large in a short-sized packet framework if the training period is not reduced. On the other hand, if the pilot length is shortened, there would be a significant degradation in performance. Since there is a trade-off between the duration of the pilot training period and the data transmission period, the main challenge is to perform a reliable channel estimation while affecting the minimal impact on the duration of data transmission period.

An aim of this paper is to propose an efficient receiver technique that exploits information obtained during the *data transmission period* to improve the reception quality of the system in the short packet transmission. Intuitively, when time resources are limited, we need to use *all* received data to optimize the receiver performance. With this goal in mind, we propose a receive filtering algorithm that estimates the interference covariance matrix using the received signal from the normal data transmission period in the IoT network. In doing so, the interference training period becomes unnecessary and the transmission rate loss caused by the interference training period can be avoided. We show from analysis and numerical experiments that the proposed method achieves a linear scaling of SINR in the number of receive antennas.

Next, we propose a low latency frame structure adequate for the one-shot random access where pilot and data are transmitted simultaneously. We propose a strategy to exploit the data symbols received from the target transmit device to improve the channel estimation quality at the receiver. There have been previous studies exploiting data signals for channel estimation including the non-OFDM system with frequencyselective channel [16], wireless LAN (IEEE 802.11n) [17], and LTE systems with long packet [18] In this paper, we choose the most reliable received data symbols, referred to as virtual pilots, among all possible soft decision data symbols and then use them to re-estimate the channel. Our proposed method is distinct from previous efforts in the sense that select a virtual pilot group making a dominant contribution to the channel estimation quality. Towards this end, we design a mean square error (MSE) based virtual pilot selection strategy. We show from numerical simulations that the proposed method outperforms the conventional receiver technique in the short packet transmission (e.g., packet size is set to tens of bytes).

The remainder of the paper is organized as follows. In Section II, we describe the structure of a packet and review conventional receiver techniques. In Section III, we present the proposed interference covariance matrix estimation

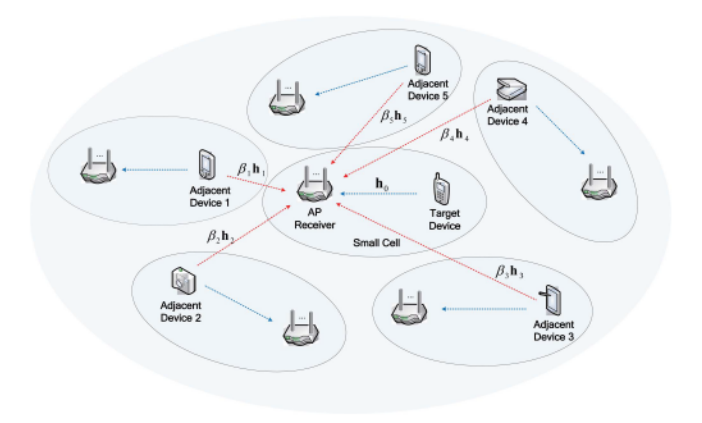


Fig. 1. A paired AP receives the desired signal from a target device and is subject to interference (dashed lines) from neighboring devices.

technique suited to the short packet transmission. In Section IV, we describe the proposed virtual pilot based channel estimation technique. In Section V, we present simulation results to verify the performance of the proposed scheme. We conclude the paper in Section VI.

We briefly summarize notation used in this paper. We employ uppercase boldface letters for matrices and lower-case boldface letters for vectors. The superscripts $(\cdot)^H$ and $(\cdot)^T$ denote the conjugate transpose and transpose, respectively. $\mathbb C$ denotes the field of complex numbers. $\|\cdot\|_p$ indicates the p-norm. $\mathbf I_N$ is the $N\times N$ identity matrix. $E[\cdot]$ is the expectation operator. \otimes is the Kronecker product operator. $\mathcal{CN}(m,\sigma^2)$ denotes a complex Gaussian random variable with mean m and variance σ^2 .

II. SYSTEM DESCRIPTION

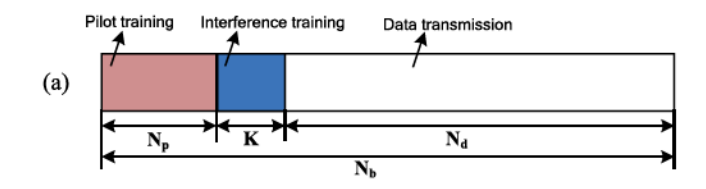
A. System Model and Packet Structure

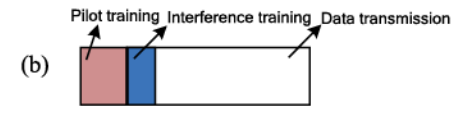
We consider uplink communication in an IoT networks such as wireless sensor networks, ad hoc network, and energy harvesting network, with an example setup shown in Fig. 1. We assume that the target transmit device has a single antenna and the paired access point (AP) receiver has N antennas. Since there are a large number of devices in the radio transmission range, the received signal contains interference from adjacent devices as well as the desired information. We assume a block-fading channel model, and each block consists of N_b channel uses, among which N_p uses are for the pilot training and N_d uses are for the data transmission (see Fig. 2(a)).

In this setup, the received signal for the ℓ -th channel use in the i-th fading block is given by

$$\mathbf{y}_{i}[\ell] = \beta_{0}\mathbf{h}_{0,i}s_{0,i}[\ell] + \sum_{j=1}^{J}\beta_{j}\mathbf{h}_{j,i}s_{j,i}[\ell] + \mathbf{n}_{i}[\ell]$$
 (1)

²In this work, we assume that the AP receiver experiences interference from devices in neighboring cells for both channel estimation phase and data transmission phase. In short packet transmission, the packet length would be far shorter than the channel coherent time and thus the channel can be fairly static and at least slowly varying within a packet. Therefore, in the short packet regime, impact of mis-aligned coherence block would not be significant. For the sake of simplicity, we assume that the coherence times of the desired channel and interfering channels are equal.





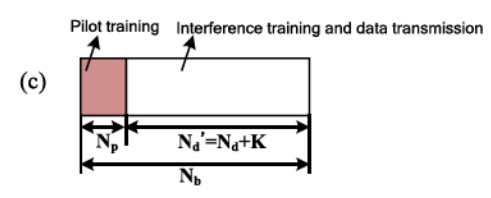


Fig. 2. Packet structure of (a) the conventional MMSE receiver for long data packets, (b) the conventional MMSE receiver for short data packets, and (c) the proposed linear receiver for short data packets.

where $\beta_0 = d_0^{-\alpha/2}$ is the attenuation factor for the target transmit device ($\beta_0 > 0$), α is the path-loss exponent ($\alpha > 2$), $\mathbf{h}_{0,i} \in \mathbb{C}^{N \times 1}$ is the channel vector between the target transmit device and AP receiver, $s_{0,i}[\ell]$ is the symbol transmitted by the target transmit device $(E[|s_{0,i}[\ell]|^2] = \rho)$, J is the number of interfering devices from neighboring cells, $\beta_j = d_j^{-\alpha/2}$ is the attenuation factor for the *j*-th interferer $(\beta_j > 0)$, $\mathbf{h}_{j,i} \in \mathbb{C}^{N \times 1}$ is the channel vector between the *j*-th interferer and AP receiver, $s_{i,i}[\ell]$ is the symbol transmitted by the j-th interferer $(E[|s_{i,i}[\ell]|^2] = \rho)$, and $\mathbf{n}_i[\ell] \in \mathbb{C}^{N \times 1}$ is the complex Gaussian noise vector $(\mathbf{n}_i[\ell] \sim \mathcal{CN}(0, \sigma^2\mathbf{I}))$. Also, without loss of generality, we assume that the distances d_0, d_1, \ldots, d_J are sorted in ascending order. In this work, we assume that the channel remains unchanged within a block and changes independently from block-to-block. In the sequel, we skip the fading block index i for notational convenience.

B. Conventional Receiver Technique

If a unit norm receive filter v is applied to the received signal vector $\mathbf{y}[\ell]$, an estimate of the desired symbol is $\hat{s}_0[\ell] = \mathbf{v}^H \mathbf{y}[\ell]$ and the resulting SINR is

$$SINR(\mathbf{v}) = \frac{\rho \mathbf{v}^H \mathbf{h}_0 \mathbf{h}_0^H \mathbf{v}}{\mathbf{v}^H (\sigma^2 \mathbf{I} + \rho \sum_{j=1}^J \beta_j \mathbf{h}_j \mathbf{h}_j^H) \mathbf{v}}.$$
 (2)

Under the condition that the target rate of the transmit device is $R = \log_2(1+\tau)$, we say a communication is successful if the received SINR is larger than τ . Hence, the outage probability at SINR threshold τ is expressed as $P_{\text{out}} = P[\text{SINR}(\mathbf{v}) \le \tau]$. Note that the receive filter \mathbf{v} can be designed to remove the interference or to boost the power of the desired signal. In order to minimize the outage probability, a receive filter weight should be designed to maximize the SINR of the receiver. This receiver is commonly dubbed as an *MMSE*

receiver [19]–[27].³ Denoting the covariance of the interference plus noise as $\Sigma = \sigma^2 \mathbf{I} + \rho \sum_j \beta_j \mathbf{h}_j \mathbf{h}_j^H$, the receive filter of the conventional MMSE receiver is [28]

$$\mathbf{v}^* = \underset{\mathbf{v}}{\operatorname{argmax}} \frac{\mathbf{v}^H \mathbf{h}_0 \mathbf{h}_0^H \mathbf{v}}{\mathbf{v}^H \Sigma \mathbf{v}} = \frac{\Sigma^{-1} \mathbf{h}_0}{\|\Sigma^{-1} \mathbf{h}_0\|_2}.$$
 (3)

Plugging (3) into (2), we obtain the best achievable SINR as

$$SINR^* = \frac{\rho (\mathbf{h}_0^H \Sigma^{-1} \mathbf{h}_0)^2}{\mathbf{h}_0^H \Sigma^{-1} (\sigma^2 \mathbf{I} + \rho \sum_{j=1}^J \beta_j \mathbf{h}_j \mathbf{h}_j^H) \Sigma^{-1} \mathbf{h}_0}$$
$$= \rho \mathbf{h}_0^H \Sigma^{-1} \mathbf{h}_0. \tag{4}$$

Note that the conventional MMSE receiver usually requires an interference training period to estimate Σ . Recall that the covariance matrix Σ is a statistic of the noise and interference. Since orthogonality among the large number of pilot sequences cannot be guaranteed, it is not easy to estimate the interfering channels \mathbf{h}_j ($j=1,\cdots,J$) individually. To handle this issue, an approach to estimate the sample covariance $\hat{\Sigma}$ using a specially designed interference training period was proposed [15]. In order to observe the covariance associated with the interference and noise, the target transmit device should remain silent in this period. The sample covariance $\hat{\Sigma}$ obtained in the interference training period is

$$\hat{\Sigma} = \frac{1}{K} \sum_{i=1}^{K} \mathbf{r}[i] \mathbf{r}[i]^{H}$$
 (5)

where K is the duration of the training period and $\mathbf{r}[i]$ is the i-th received sample $(\mathbf{r}[i] = \sum_{i=1}^{J} \beta_j \mathbf{h}_j s_j[i] + \mathbf{n}[i])$.

By replacing Σ with $\hat{\Sigma}$ in (3), i.e., using $\hat{v} = \frac{\hat{\Sigma}^{-1}h_0}{\|\hat{\Sigma}^{-1}h_0\|_2}$ instead of v^* , we obtain the SINR estimate

$$SINR = \frac{\rho \left(\mathbf{h}_0^H \hat{\Sigma}^{-1} \mathbf{h}_0\right)^2}{\mathbf{h}_0^H \hat{\Sigma}^{-H} \Sigma \hat{\Sigma}^{-1} \mathbf{h}_0}.$$
 (6)

Using a Gaussian approximation for the interference,⁴ the expected SINR⁵ of (6) becomes [29]

$$E_{\hat{\Sigma}}[SINR] = E_{\hat{\Sigma}} \left[\frac{\rho (\mathbf{h}_0^H \hat{\Sigma}^{-1} \mathbf{h}_0)^2}{\mathbf{h}_0^H \hat{\Sigma}^{-H} \Sigma \hat{\Sigma}^{-1} \mathbf{h}_0} \right]$$
$$= \left(1 - \frac{N-1}{K+1} \right) SINR^*. \tag{7}$$

Note that the expected SINR in (7) contains an additional scaling factor $1 - \frac{N-1}{K+1}$. Since the interference training period K

³The conventional performance measures such as ergodic capacity may not be suitable for short-packet communication systems because these metrics pertain to the asymptotic regime of long data packets [10], [11]. Nonetheless, this quantity is still simple and useful tool to analyze the behavior of the proposed scheme.

⁴Gaussian approximation of interferences becomes more accurate when the density of machine-type devices becomes higher.

⁵Since the average analysis is relevant only if there are sufficiently many packets, the expected SINR might not be an ideal metric for the short packet based communication systems. Nevertheless, unless the packet length is extremely short, hundreds of samples might be used in the computation of the expected SINR and thus average SINR is still meaningful.

for the short packet framework would be very small, E[SINR] would be much smaller than $SINR^*$, the best achievable SINR in (4). Further, when the number of antennas N increases, there would also be a loss in the SINR and achievable rate, which makes this approach unsuitable for the small packet transmission.

III. RECEIVER DESIGN

Recall that two main ingredients of the receive filter in (3) are the channel vector \mathbf{h}_0 and the covariance matrix Σ of the interference and noise. In this section, we present a strategy to estimate the covariance matrix Σ using measurements in the data transmission period and show that the achievable SINR of this strategy equals SINR*. By estimating the covariance matrix in the normal data transmission period instead of the interference training period, we can avoid the transmission rate loss caused by the interference training period.

Note that the received signal $\mathbf{y}[\ell] = \mathbf{h}_0 \ s_0[\ell] + \sum_{j=1}^J \beta_j \mathbf{h}_j s_j[\ell] + \mathbf{n}[\ell]$ contains interference from adjacent devices and noise as well as the desired signal. Using the receive filter $\mathbf{v} = \frac{\Sigma_0^{-1} \mathbf{h}_0}{\|\Sigma_0^{-1} \mathbf{h}_0\|_2}$, the estimate of the desired symbol becomes

$$\hat{s}_{0}[\ell] = \mathbf{v}^{H} \mathbf{y}[\ell]
= \frac{\rho \mathbf{h}_{0}^{H} (\rho \mathbf{h}_{0} \mathbf{h}_{0}^{H} + \rho \sum_{j=1}^{J} \beta_{j} \mathbf{h}_{j} \mathbf{h}_{j}^{H} + \sigma^{2} \mathbf{I})^{-1}}{\|\rho \mathbf{h}_{0}^{H} (\rho \mathbf{h}_{0} \mathbf{h}_{0}^{H} + \rho \sum_{j=1}^{J} \beta_{j} \mathbf{h}_{j} \mathbf{h}_{j}^{H} + \sigma^{2} \mathbf{I})^{-1}\|_{2}} \mathbf{y}[\ell]
= \frac{\mathbf{h}_{0}^{H} \sum_{0}^{-1}}{\|\mathbf{h}_{0}^{H} \sum_{0}^{-1}\|_{2}} \mathbf{y}[\ell]$$
(8)

where $\Sigma_0 = \Sigma + \rho \mathbf{h}_0 \mathbf{h}_0^H$. In the following theorem, we show that the best possible SINR in (4) can be achieved even with the inclusion of the desired signal in the covariance matrix.⁶

Theorem 1: When the covariance matrix Σ_0 is employed in the receive filter $\mathbf{v} = \frac{\Sigma_0^{-1}\mathbf{h}_0}{\|\Sigma_0^{-1}\mathbf{h}_0\|_2}$, the SINR of the proposed strategy is $\mathrm{SINR}^* = \rho\mathbf{h}_0^H \, \Sigma^{-1}\mathbf{h}_0$.

Proof: Let SINR_{prop} be the SINR of the proposed strategy. Then, using (2), we have

$$SINR_{prop} = \frac{\rho \left(\mathbf{h}_0^H \left(\Sigma + \rho \mathbf{h}_0 \mathbf{h}_0^H\right)^{-1} \mathbf{h}_0\right)^2}{\mathbf{h}_0^H \left(\Sigma + \rho \mathbf{h}_0 \mathbf{h}_0^H\right)^{-1} \Sigma \left(\Sigma + \rho \mathbf{h}_0 \mathbf{h}_0^H\right)^{-1} \mathbf{h}_0}.$$
 (9)

We first consider the numerator. Using the matrix inversion lemma, 7 we have

$$\left(\Sigma + \rho \mathbf{h}_0 \mathbf{h}_0^H\right)^{-1} = \Sigma^{-1} - \frac{\Sigma^{-1} \mathbf{h}_0 \mathbf{h}_0^H \Sigma^{-1}}{\rho + \mathbf{h}_0^H \Sigma^{-1} \mathbf{h}_0}.$$
 (10)

⁶In this section, we focus on the effect of covariance matrix Σ_0 and the sample covariance matrix $\hat{\Sigma}_0$ on SINR under the assumption that \mathbf{h}_0 is perfectly known at the receiver. We discuss the effect of estimated channel $\hat{\mathbf{h}}_0$ in the next section.

The first a large part of the first and the first and the first and I in the next section. The first and I is the matrix inversion lemma I in the matrix inversion lemma I in the first and I in the matrix inversion lemma I in the first and I in the matrix inversion lemma I in the first and I in the matrix inversion lemma I in the first and I in the first and I in the matrix inversion lemma I in the first and I in the matrix inversion lemma I in the first and I in the matrix inversion lemma I in the first and I in the matrix inversion lemma I

From (9) and (10), we have

$$\left(\mathbf{h}_{0}^{H} \left(\Sigma + \rho \mathbf{h}_{0} \mathbf{h}_{0}^{H}\right)^{-1} \mathbf{h}_{0}\right)^{2} \\
= \left(\mathbf{h}_{0}^{H} \Sigma^{-1} \mathbf{h}_{0} - \frac{(\mathbf{h}_{0}^{H} \Sigma^{-1} \mathbf{h}_{0})^{2}}{\rho + \mathbf{h}_{0}^{H} \Sigma^{-1} \mathbf{h}_{0}}\right)^{2} \\
= \left(\frac{\rho \mathbf{h}_{0}^{H} \Sigma^{-1} \mathbf{h}_{0}}{\rho + \mathbf{h}_{0}^{H} \Sigma^{-1} \mathbf{h}_{0}}\right)^{2} = \left(\frac{\rho \text{SINR}^{*}}{\rho^{2} + \text{SINR}^{*}}\right)^{2} (11)$$

where SINR* = $\rho \mathbf{h}_0^H \Sigma^{-1} \mathbf{h}_0$ (see (4)). Now, by plugging (10) into the denominator of (9), we have

$$\mathbf{h}_{0}^{H} \left(\Sigma + \rho \mathbf{h}_{0} \mathbf{h}_{0}^{H}\right)^{-1} \Sigma \left(\Sigma + \rho \mathbf{h}_{0} \mathbf{h}_{0}^{H}\right)^{-1} \mathbf{h}_{0}$$

$$= \mathbf{h}_{0}^{H} \left(\Sigma^{-1} - \frac{\Sigma^{-1} \mathbf{h}_{0} \mathbf{h}_{0}^{H} \Sigma^{-1}}{\rho + \mathbf{h}_{0}^{H} \Sigma^{-1} \mathbf{h}_{0}}\right) \Sigma \left(\Sigma^{-1} - \frac{\Sigma^{-1} \mathbf{h}_{0} \mathbf{h}_{0}^{H} \Sigma^{-1}}{\rho + \mathbf{h}_{0}^{H} \Sigma^{-1} \mathbf{h}_{0}}\right) \mathbf{h}_{0}$$

$$= \left(\mathbf{h}_{0}^{H} - \frac{\mathbf{h}_{0}^{H} \Sigma^{-1} \mathbf{h}_{0} \mathbf{h}_{0}^{H}}{\rho + \mathbf{h}_{0}^{H} \Sigma^{-1} \mathbf{h}_{0}}\right) \left(\Sigma^{-1} \mathbf{h}_{0} - \frac{\Sigma^{-1} \mathbf{h}_{0} \mathbf{h}_{0}^{H} \Sigma^{-1} \mathbf{h}_{0}}{\rho + \mathbf{h}_{0}^{H} \Sigma^{-1} \mathbf{h}_{0}}\right)$$

$$= \frac{\rho^{2} \mathbf{h}_{0}^{H} \Sigma^{-1} \mathbf{h}_{0}}{\left(\rho + \mathbf{h}_{0}^{H} \Sigma^{-1} \mathbf{h}_{0}\right)^{2}} = \frac{\rho^{3} \text{SINR}^{*}}{\left(\rho^{2} + \text{SINR}^{*}\right)^{2}}.$$
(12)

Plugging (11) and (12) into (9), we have

$$SINR_{prop} = \frac{\rho \left(\frac{\rho SINR^*}{\rho^2 + SINR^*}\right)^2}{\frac{\rho^3 SINR^*}{(\rho^2 + SINR^*)^2}} = SINR^*, \tag{13}$$

which is the desired result.

It is worth noting that the main goal of Theorem 1 is to validate the method of estimating the covariance matrix in using only normal data transmission. By achieving the maximum SINR and avoiding the interference training period, the proposed method can exploit an additional *K* channel uses for the data transmission period compared to the conventional MMSE receiver.

By slightly modifying this result and using a Gaussian approximation for the interference, we can obtain the SINR expression for a realistic scenario where the sample covariance matrix is employed. In this scenario, we use $\hat{\Sigma}_0 = \hat{\Sigma} + \rho \hat{\mathbf{h}}_0 \hat{\mathbf{h}}_0^H$ instead of Σ_0 , and thus the modified receive filter is⁸

$$\hat{\mathbf{v}} = \frac{\hat{\Sigma}_0^{-1} \mathbf{h}_0}{\|\hat{\Sigma}_0^{-1} \mathbf{h}_0\|_2}.$$
 (14)

Theorem 2: When the sample covariance in (14) is employed, the expected SINR of the proposed linear MMSE receiver is

$$E_{\hat{\Sigma}_{0}}[SINR_{prop}] = E_{\hat{\Sigma}_{0}} \left[\frac{\rho (\mathbf{h}_{0}^{H} \hat{\Sigma}_{0}^{-1} \mathbf{h}_{0})^{2}}{\mathbf{h}_{0}^{H} \hat{\Sigma}_{0}^{-1} \Sigma \hat{\Sigma}_{0}^{-1} \mathbf{h}_{0}} \right]$$
$$= \left(1 - \frac{N-1}{N_{d}+1} \right) SINR^{*}. \tag{15}$$

 $^8 Here$ we use \hat{h}_0 instead of $h_0 in~\hat{\Sigma}_0$ in order to observe the effect of $\hat{\Sigma}_0$ on SINR.

Proof: By the direct substitution of $\hat{\Sigma}_0 = \hat{\Sigma} + \rho \hat{\mathbf{h}}_0 \hat{\mathbf{h}}_0^H$ into (6), we have

SINR =
$$\frac{\left(\mathbf{h}_{0}^{H} \hat{\Sigma}_{0}^{-1} \mathbf{h}_{0}\right)^{2}}{\left(\mathbf{h}_{0}^{H} \hat{\Sigma}_{0}^{-1} \Sigma \hat{\Sigma}_{0}^{-1} \mathbf{h}_{0}\right)}.$$
 (16)

Let $\widetilde{\Sigma} = \hat{\Sigma} + \rho (\hat{\mathbf{h}}_0 \hat{\mathbf{h}}_0^H - \mathbf{h}_0 \mathbf{h}_0^H)$, then $\hat{\Sigma}_0 = \widetilde{\Sigma} + \rho \mathbf{h}_0 \mathbf{h}_0^H$ and $\hat{\Sigma}_0^{-1} = \widetilde{\Sigma}^{-1} - \frac{\widetilde{\Sigma}^{-1} \mathbf{h}_0 \mathbf{h}_0^H \widetilde{\Sigma}^{-1}}{\rho + \mathbf{h}_0^H \widetilde{\Sigma}^{-1} \mathbf{h}_0}$ by the matrix inversion lemma. Therefore,

SINR =
$$\frac{\rho \left(\mathbf{h}_{0}^{H} \left(\widetilde{\Sigma}^{-1} - \frac{\widetilde{\Sigma}^{-1}\mathbf{h}_{0}\mathbf{h}_{0}^{H}\widetilde{\Sigma}^{-1}}{\rho + \mathbf{h}_{0}^{H}\widetilde{\Sigma}^{-1}\mathbf{h}_{0}}\right) \mathbf{h}_{0}\right)^{2}}{\left(\mathbf{h}_{0}^{H} \left(\widetilde{\Sigma}^{-1} - \frac{\widetilde{\Sigma}^{-1}\mathbf{h}_{0}\mathbf{h}_{0}^{H}\widetilde{\Sigma}^{-1}}{\rho + \mathbf{h}_{0}^{H}\widetilde{\Sigma}^{-1}\mathbf{h}_{0}}\right) \Sigma \left(\widetilde{\Sigma}^{-1} - \frac{\widetilde{\Sigma}^{-1}\mathbf{h}_{0}\mathbf{h}_{0}^{H}\widetilde{\Sigma}^{-1}}{\rho + \mathbf{h}_{0}^{H}\widetilde{\Sigma}^{-1}\mathbf{h}_{0}}\right) \mathbf{h}_{0}\right)}$$

$$= \frac{\rho \left(\frac{\rho \mathbf{h}_{0}^{H}\widetilde{\Sigma}^{-1}\mathbf{h}_{0}}{\rho + \mathbf{h}_{0}^{H}\widetilde{\Sigma}^{-1}\mathbf{h}_{0}}\right)^{2}}{\left(\frac{\rho^{2}\mathbf{h}_{0}^{H}\widetilde{\Sigma}^{-1}\Sigma\widetilde{\Sigma}^{-1}\mathbf{h}_{0}}{(\rho + \mathbf{h}_{0}^{H}\widetilde{\Sigma}^{-1}\mathbf{h}_{0})^{2}}\right)} = \frac{\rho \left(\mathbf{h}_{0}^{H}\widetilde{\Sigma}^{-1}\mathbf{h}_{0}\right)^{2}}{\mathbf{h}_{0}^{H}\widetilde{\Sigma}^{-1}\Sigma\widetilde{\Sigma}^{-1}\mathbf{h}_{0}}.$$
(17)

Further, by denoting $\kappa = \frac{\text{SINR}}{\text{SINR}^*}$, $\Xi = (\frac{\text{SINR}^*}{\rho})^{-\frac{1}{2}} \Sigma^{-\frac{1}{2}} \mathbf{h}_0$, and $\hat{\Sigma}_1 = \Sigma^{-\frac{1}{2}} \widetilde{\Sigma} \Sigma^{-\frac{1}{2}}$, we have

$$\kappa = \frac{1}{\text{SINR}^*} \frac{\rho \left(\mathbf{h}_0^H \tilde{\Sigma}^{-1} \mathbf{h}_0 \right)^2}{\mathbf{h}_0^H \tilde{\Sigma}^{-1} \Sigma \tilde{\Sigma}^{-1} \mathbf{h}_0}$$
$$= \frac{\left(\Xi^H \hat{\Sigma}_1^{-1} \Xi \right)^2}{\Xi^H \hat{\Sigma}_1^{-2} \Xi}.$$
 (18)

Note that the joint distribution of the elements of $\hat{\Sigma}$ follows the central complex Wishart distribution $CW(M,N;\Sigma)$ [30]. Hence, $E[\hat{\Sigma}_1] = \Sigma^{-\frac{1}{2}}E[\tilde{\Sigma}]\Sigma^{-\frac{1}{2}} = \Sigma^{-\frac{1}{2}}\Sigma\Sigma^{-\frac{1}{2}} = \mathbf{I}$, and $\hat{\Sigma}_1$ is a complex Wishart distribution $CW(N_d,N;\mathbf{I})$. The probability density function of κ is given by [29]

$$P(\kappa) = \frac{\Gamma(N_d + 1)}{\Gamma(N - 1)\Gamma(N_d + 2 - N)} \kappa^{(N_d + 2 - N) - 1}$$

$$(1 - \kappa)^{(N - 1) - 1}$$
(19)

where κ follows the regularized incomplete beta distribution. Since $\Gamma(i) = (i-1)!$ for an integer i, the expectation of κ is

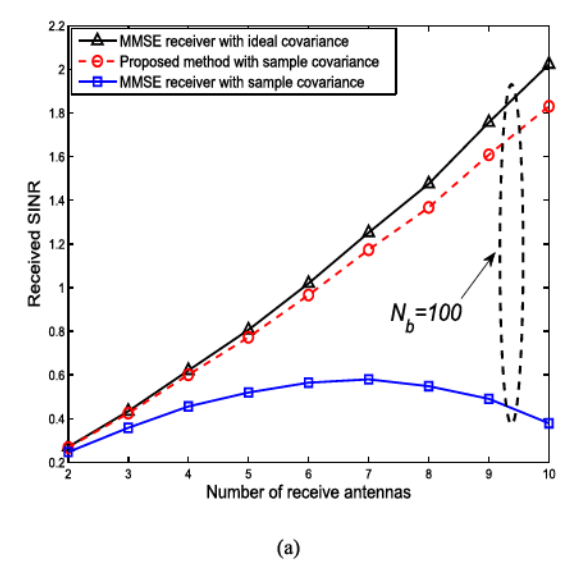
$$E[\kappa] = \int_0^1 \kappa P(\kappa) d\kappa$$

$$= \frac{N_d!}{(N_d - 2)!(N_d + 1 - N)!} \int_0^1 \kappa^{N_d + 2 - N} (1 - \kappa)^{N - 2} d\kappa$$

$$= 1 - \frac{N - 1}{N_d + 1}.$$
(20)

Recalling that $\kappa = \frac{1}{\text{SINR}^*} \frac{\rho \left(\mathbf{h}_0^H \hat{\Sigma}_0^{-1} \mathbf{h}_0 \right)^2}{\mathbf{h}_0^H \hat{\Sigma}_0^{-1} \mathbf{\Sigma} \hat{\Sigma}_0^{-1} \mathbf{h}_0}$, we further have

$$\begin{split} E_{\hat{\Sigma}_0} \left[\text{SINR}_{\text{prop}} \right] &= E_{\hat{\Sigma}_0} \left[\frac{\rho \ (\mathbf{h}_0^H \hat{\Sigma}_0^{-1} \mathbf{h}_0)^2}{\mathbf{h}_0^H \hat{\Sigma}_0^{-1} \Sigma \hat{\Sigma}_0^{-1} \mathbf{h}_0} \right] \\ &= \left(1 - \frac{N-1}{N_d+1} \right) \text{SINR}^*. \end{split}$$



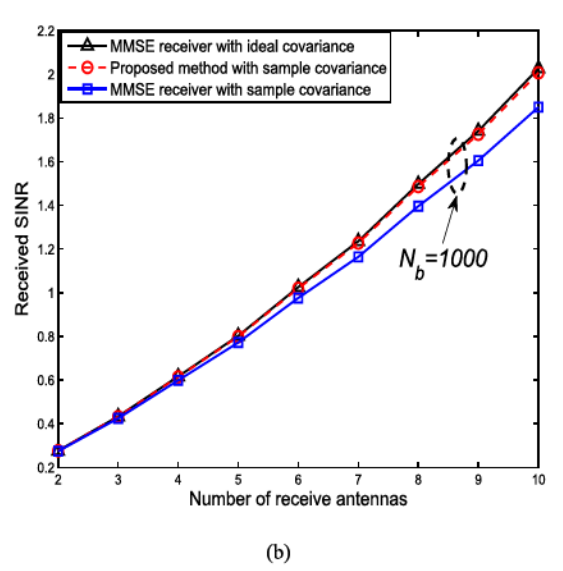


Fig. 3. The received SINR of the proposed method and conventional MMSE receiver for $N_b = 100$ and 1000. We set J = 30, SNR = 0 dB, $N_p = 0.1N_b$, $K = 0.1N_b$, $N_d = 0.8N_b$, $N_d' = 0.9N_b$.

Since the interference training period is unnecessary, the data transmission period is improved from N_d to $N'_d = N_d + K$ and at the same time the covariance matrix is estimated using samples in the data transmission period (see Fig. 2). Therefore, we obtain a more accurate estimation of the interference covariance in the short packet framework. The effect of the sample covariance matrix on the received SINR shows the efficacy of the proposed receiver by obtaining a larger scaling factor $\left(1 - \frac{N-1}{N'_d+1}\right)$. In Fig. 3, we plot the received SINR as a function of the number of receive antennas N. When the packet size N_b is large (e.g., $N_b = 1000$), which corresponds to the packet length of current wireless systems, $K = 0.1N_b$ is also sufficiently larger than the number of antennas N so that scaling factor of the proposed scheme $\left(1-\frac{N-1}{N'+1}\right)$ and the conventional MMSE receiver $\left(1-\frac{N-1}{K+1}\right)$ are not much different. This behavior, however, does not hold true for short-sized packet regime. In fact, as shown in Fig. 3(a), we see that the performance of the proposed scheme improves linearly with N. Since the interference training is needed for the conventional MMSE receiver, we observe that when N_b is small (e.g., $N_b = 100$) the performance of the conventional MMSE SINR receiver with sample covariance matrix does not scale with N.

IV. JOINT PILOT AND DATA SYMBOL BASED CHANNEL ESTIMATION

In the previous sections, we assumed that the desired channel \mathbf{h}_0 is perfectly known. As mentioned, when we consider the short packet transmission, the training period should also be reduced to avoid an excessive amount of training overhead. In this section, we propose a channel estimation technique that jointly uses the pilot signals and data symbols to improve channel estimation quality. In a nutshell, the proposed channel estimation technique picks a small number of reliable data symbols among all available data symbols.

Using the chosen data symbols (which we call *virtual pilots*) together with the pilot signals in the re-estimation of the channel vector, we achieve great improvement of the channel estimation performance in the short packet regime.

A. The Joint Pilot and Data Symbol Based Channel Estimation

Before we proceed, we briefly review conventional MMSEbased channel estimation. The received pilot signals in the training period are expressed as

$$\mathbf{y}^{(1)} = \mathbf{h}_0 p_0^{(1)} + \sum_{j=1}^{J} \beta_j \mathbf{h}_j s_j^{(1)} + \mathbf{n}^{(1)}$$

$$\vdots$$

$$\mathbf{y}^{(N_p)} = \mathbf{h}_0 p_0^{(N_p)} + \sum_{j=1}^{J} \beta_j \mathbf{h}_j s_j^{(N_p)} + \mathbf{n}^{(N_p)}$$
(21)

where $\mathbf{y}^{(i)}$ is the *i*-th observation, $\mathbf{n}^{(i)}$ is the *i*-th noise, $p_0^{(i)}$ is the *i*-th pilot signal in the target transmit device, and N_p is the total number of pilot observations. The $N_pN \times 1$ vectorized received pilot signals are

$$\mathbf{y}_p = \mathbf{P}_0 \mathbf{h}_0 + \mathbf{z}_p \tag{22}$$

where $\mathbf{P}_0 = \mathbf{p}_0 \otimes \mathbf{I}_N$ is $N_p N \times N$ -dimensional training matrix with $\mathbf{p}_0 = [p_0^{(1)}, \dots, p_0^{(N_p)}]^T$, and $\mathbf{z}_p = [(\sum_{j=1}^J \beta_j \mathbf{h}_j s_j^{(1)} + \mathbf{n}^{(1)})^T \cdots (\sum_{j=1}^J \beta_j \mathbf{h}_j s_j^{(N_p)} + \mathbf{n}^{(N_p)})^T]^T$ is the interference plus noise vector over the training period. We assume that \mathbf{h}_0 follows a circular symmetric complex normal distribution, i.e., $\mathbf{h}_0 \sim \mathcal{CN}(\mathbf{0}, \mathbf{C}_{hh})$ where $\mathbf{C}_{hh} = \mathbf{Cov}(\mathbf{h}_0, \mathbf{h}_0)$. The MMSE weight matrix minimizing the mean square error between the original channel vector \mathbf{h}_0 and the estimate $\hat{\mathbf{h}}_0 = \mathbf{W}_{\mathbf{V}_p}$ is [31]

$$W = \text{Cov} (\mathbf{h}_{0}, \mathbf{y}_{p}) \text{Cov} (\mathbf{y}_{p}, \mathbf{y}_{p})^{-1}$$

$$= E[\mathbf{h}_{0}\mathbf{y}_{p}^{H}] E[\mathbf{y}_{p}\mathbf{y}_{p}^{H}] \qquad (23)$$

$$= E[\mathbf{h}_{0}\mathbf{h}_{0}^{H}\mathbf{P}_{0}^{H} + \mathbf{h}_{0}\mathbf{z}_{p}^{H}]$$

$$\times E[\mathbf{P}_{0}\mathbf{h}_{0}\mathbf{h}_{0}^{H}\mathbf{P}_{0}^{H} + \mathbf{P}_{0}\mathbf{h}_{0}\mathbf{z}_{p}^{H} + \mathbf{z}_{p}\mathbf{h}_{0}^{H}\mathbf{P}_{0}^{H} + \mathbf{z}_{p}\mathbf{z}_{p}^{H}]$$

$$= \mathbf{C}_{hh}\mathbf{P}_{0}^{H} \left(\mathbf{P}_{0}\mathbf{C}_{hh}\mathbf{P}_{0}^{H} + \eta_{p}\mathbf{I}_{N}\right)^{-1} \qquad (24)$$

where (23) is due to $Cov(\mathbf{a}, \mathbf{b}) = E[\mathbf{a}\mathbf{b}^H] - E[\mathbf{a}]E[\mathbf{b}^H]$ and η_p is the variance of the interference plus noise. The corresponding MMSE-based channel estimate $\hat{\mathbf{h}}_0$ is

$$\hat{\mathbf{h}}_{0} = \mathbf{C}_{hh} \mathbf{P}_{0}^{H} \left(\mathbf{P}_{0} \mathbf{C}_{hh} \mathbf{P}_{0}^{H} + \eta_{p} \mathbf{I}_{N} \right)^{-1} \left(\mathbf{P}_{0} \mathbf{h}_{0} + \mathbf{z}_{p} \right)
= (N_{p} \mathbf{C}_{hh} + \eta_{p} \mathbf{I}_{N})^{-1} \mathbf{C}_{hh} \mathbf{P}_{0}^{H} (\mathbf{P}_{0} \mathbf{h}_{0} + \mathbf{z}_{p})
= \left(\frac{\eta_{p}}{N_{p}} \mathbf{I}_{N} + \mathbf{C}_{hh} \right)^{-1} \mathbf{C}_{hh} \left(\mathbf{h}_{0} + \frac{1}{N_{p}} \mathbf{P}_{0}^{H} \mathbf{z}_{p} \right).$$
(25)

We observe from (25) that the estimated channel vector $\hat{\mathbf{h}}_0$ converges to the original channel vector \mathbf{h}_0 as the training period N_p increases. This clearly demonstrates that there would be a degradation in the channel estimation quality for the short packet regime. To enhance the channel estimation quality without increasing the pilot overhead, we exploit the virtual pilots in the re-estimation of channels. Using the deliberately chosen virtual pilots together with the conventional pilots, the channel is re-estimated, and the newly generated channel estimate will be used for the symbol detection. When N_v data symbols are selected for the virtual pilot purpose, the received signals are

$$\mathbf{y}^{(1)} = \mathbf{h}_0 s_0^{(1)} + \sum_{j=1}^J \beta_j \mathbf{h}_j s_j^{(1)} + \mathbf{n}^{(1)}$$

$$\vdots$$

$$\mathbf{y}^{(N_v)} = \mathbf{h}_0 s_0^{(N_v)} + \sum_{i=1}^J \beta_j \mathbf{h}_j s_j^{(N_v)} + \mathbf{n}^{(N_v)}$$
(26)

where $\mathbf{y}^{(i)}$ is the *i*-th observation, $\mathbf{n}^{(i)}$ is the *i*-th noise, $s_0^{(i)}$ is the data symbol of the target transmit device, and $s_j^{(i)}$ is the data symbol of the *j*-th interferer. The $N_v N \times 1$ vectorized virtual pilot observations can be expressed as

$$\mathbf{v}_p = \mathbf{S}_0 \mathbf{h}_0 + \mathbf{z}_p \tag{27}$$

where $\mathbf{S}_0 = \mathbf{s}_0 \otimes \mathbf{I}_N$ (of size $N_v N \times N$) is the virtual pilot matrix where $\mathbf{s}_0 = [s_0^{(1)}, \dots, s_0^{(N_v)}]^T$ is the data symbol sequence and $\mathbf{z}_v = \left[(\sum_{j=1}^J \beta_j \mathbf{h}_j s_j^{(1)} + \mathbf{n}^{(1)})^T \cdots \right]$

 $\left(\sum_{j=1}^{J} \beta_{j} \mathbf{h}_{j} s_{j}^{(N_{v})} + \mathbf{n}^{(N_{v})}\right)^{T}$ is the interference plus noise signal vector in the virtual pilot transmission period. By stacking the pilot observation vector \mathbf{y}_{p} and virtual pilot observation vector \mathbf{y}_{v} , we obtain the composite observation vector \mathbf{y}_{c} for the channel re-estimation as

$$\mathbf{y}_c = \begin{bmatrix} \mathbf{y}_p \\ \mathbf{v}_n \end{bmatrix} = \begin{bmatrix} \mathbf{P}_0 \\ \mathbf{S}_0 \end{bmatrix} \mathbf{h}_0 + \begin{bmatrix} \mathbf{z}_p \\ \mathbf{z}_n \end{bmatrix}. \tag{28}$$

The MMSE estimate of the proposed scheme is expressed as

$$\hat{\mathbf{h}}_0 = \operatorname{Cov}(\mathbf{h}_0, \mathbf{y}_c) \operatorname{Cov}(\mathbf{y}_c, \mathbf{y}_c)^{-1} \mathbf{y}_c
= \mathbf{\Omega} \mathbf{\Sigma}^{-1} \mathbf{v}_c$$
(29)

⁹Since it is hard to obtain exact variance $\sum_{j=1}^{J} \beta_{j}^{2} N \rho + \sigma^{2}$, we instead use $\eta_{\rm p} = J \bar{\beta}^{2} N \rho + \sigma^{2}$ where $\bar{\beta} = \bar{d}^{\alpha/2}$ is obtained by using the cell-radius \bar{d} under the assumption that the interferers are closer to the receiver (i.e., $\bar{\beta} > \beta_{j}$). Thus, the channel estimation might be slightly pessimistic. Also, the reason to treat interference as noise in (24) is because it is difficult to acquire the covariance of the interference. Note that the MSE formula in (37) is obtained under the assumption that h_{0} as well as the interfering channels are spatially uncorrelated.

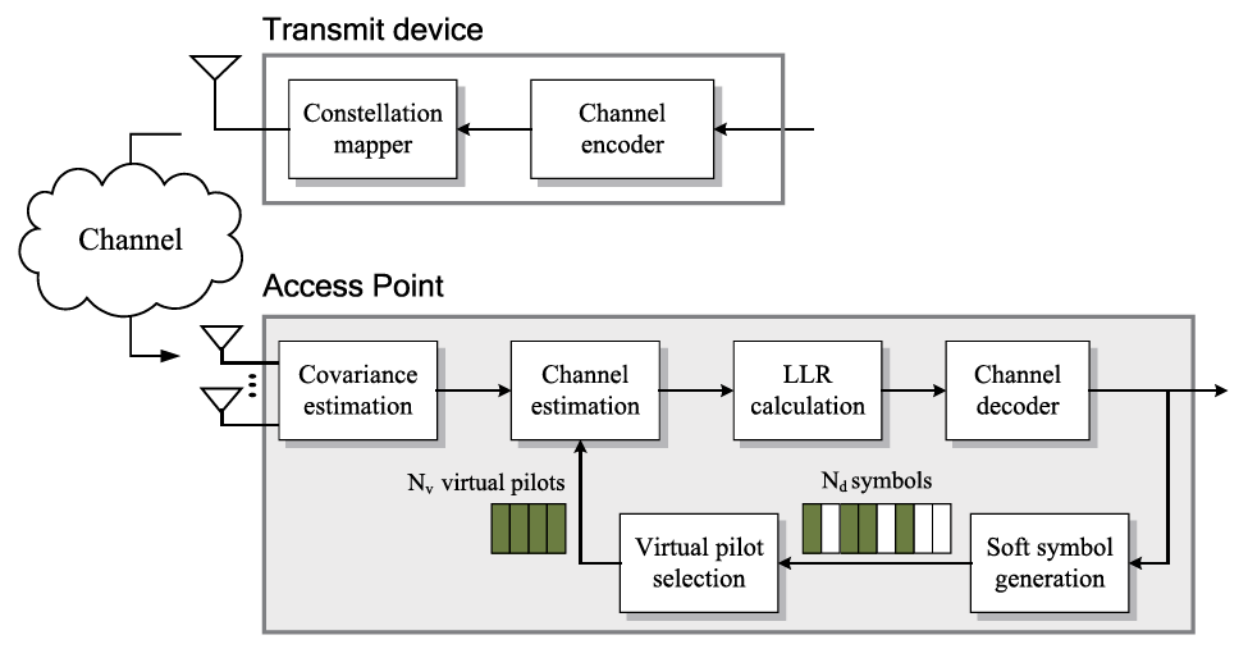


Fig. 4. Block diagram of the receiver using virtual pilot and pilot signal in the re-estimation of the channel. Among all the data symbols, symbols with small MSE are chosen as virtual pilots. Note that symbols with small MSE are green colored.

where

$$\Omega = \operatorname{Cov}(\mathbf{h}_0, \mathbf{y}_c)
= \left[E[\mathbf{h}_0 \mathbf{y}_p^H] \quad E[\mathbf{h}_0 \mathbf{y}_v^H] \right] = \left[\mathbf{C}_{hh} \mathbf{P}_0^H \quad \mathbf{C}_{hh} \bar{\mathbf{S}}_0^H \right] (30)$$

and

$$\Sigma = \operatorname{Cov}(\mathbf{y}_{c}, \mathbf{y}_{c})$$

$$= \begin{bmatrix} E[\mathbf{y}_{p}\mathbf{y}_{p}^{H}] & E[\mathbf{y}_{p}\mathbf{y}_{v}^{H}] \\ E[\mathbf{y}_{v}\mathbf{y}_{p}^{H}] & E[\mathbf{y}_{v}\mathbf{y}_{v}^{H}] \end{bmatrix}$$

$$= \begin{bmatrix} \mathbf{P}_{0}\mathbf{C}_{hh}\mathbf{P}_{0}^{H} + \eta_{p}\mathbf{I} & \mathbf{P}_{0}\mathbf{C}_{hh}\bar{\mathbf{S}}_{0}^{H} \\ \bar{\mathbf{S}}_{0}\mathbf{C}_{hh}\mathbf{P}_{0}^{H} & \mathbf{\Lambda}_{0} \otimes \operatorname{diag}(\mathbf{C}_{hh}) + \eta_{v}\mathbf{I} \end{bmatrix}. (31)$$
that $\bar{\mathbf{S}}_{v} = E[\mathbf{S}_{v}] = \bar{\mathbf{S}}_{v} + \mathbf{S}_{v} = \mathbf$

Note that $\bar{\mathbf{S}}_0 = E[\mathbf{S}_0] = \bar{\mathbf{s}}_0 \otimes \mathbf{I}_N$ where $\bar{\mathbf{s}}_0 = [\bar{s}_0^{(1)}, \dots, \bar{s}_0^{(N_b)}]^T$ is obtained from the first order moment of $s_0^{(i)}$ [32]. That is,

$$\bar{s}_0^{(i)} = E[s_0^{(i)}] = \sum_{\theta \in \Theta} \theta \prod_{k=1}^{Q} \frac{1}{2} \left(1 + c_{0,k}^{(i)} \tanh\left(\frac{1}{2}L(c_{0,k}^{(i)})\right) \right)$$
(32)

where Θ is a constellation set, $c_{0,k}^{(i)}$ is the k-th coded bit, Q is the number of (coded) bits mapped to a data symbol $s_0^{(i)}$ in 2^Q -ary quadrature amplitude modulation (QAM) constellations, and $L(c_{0,k}^{(i)})$ is the log-likelihood ratio (LLR) of the k-th coded bit mapped from a data symbol $s_0^{(i)}$. $\Lambda_0 =$ $[\bar{\lambda}_0^{(1)},\ldots,\bar{\lambda}_0^{(N_v)}]^T$ is the vector of the second order moments of $s_0^{(i)}$ given by

$$\begin{split} \bar{\lambda}_0^{(i)} &= E[|s_0^{(i)}|^2] \\ &= \sum_{\theta \in \Theta} |\theta|^2 \prod_{k=1}^{Q} \frac{1}{2} \left(1 + c_{0,k}^{(i)} \tanh\left(\frac{1}{2} L(c_{0,k}^{(i)})\right) \right). \end{split} \tag{33}$$

Plugging (29) and (30) into (28), we obtain the channel estimate $\hat{\mathbf{h}}_0$ as

$$\begin{split} \hat{\mathbf{h}}_0 &= \begin{bmatrix} \mathbf{C}_{hh} \mathbf{P}_0^H & \mathbf{C}_{hh} \bar{\mathbf{S}}_0^H \end{bmatrix} \\ &\times \begin{bmatrix} \mathbf{P}_0 \mathbf{C}_{hh} \mathbf{P}_0^H + \eta_p \mathbf{I} & \mathbf{P}_0 \mathbf{C}_{hh} \bar{\mathbf{S}}_0^H \\ \bar{\mathbf{S}}_0 \mathbf{C}_{hh} \mathbf{P}_0^H & \mathbf{\Lambda}_0 \otimes \operatorname{diag}(\mathbf{C}_{hh}) + \eta_v \mathbf{I} \end{bmatrix}^{-1} \begin{bmatrix} \mathbf{y}_p \\ \mathbf{y}_v \end{bmatrix} . \end{split} \\ &= \operatorname{tr} \left(\operatorname{Cov} \left(\mathbf{h}_0 \right) - \operatorname{Cov} \left(\tilde{\mathbf{\Omega}} \tilde{\mathbf{\Sigma}}^{-1} \begin{bmatrix} \mathbf{y}_p \\ \mathbf{y}_v^{(n)} \end{bmatrix} \right) \right) \end{split}$$

While the conventional MMSE estimate in (25) uses only the received pilot sequence for the channel estimation, the proposed channel estimator in (29) utilizes the most reliable data symbols, i.e., the soft symbol estimate \bar{S}_0 and second order moments Λ_0 , as virtual pilots. Clearly, reliability of the soft symbols directly affects the quality of the proposed channel estimation so that we need to choose virtual pilots with caution.

B. Virtual Pilot Selection

Since the virtual pilots can improve the channel estimation quality of the proposed method, the best way to select virtual pilots would be to compare the performance metric (e.g., MSE of the estimated channel) of all possible $\binom{N_d}{N_n}$ data symbol combinations and then choose the combination achieving the minimum MSE. Since this procedure is computationally demanding and hence not pragmatic, we use a simple suboptimal approach to compute the MSE when single data symbol is used for the virtual pilot. Among all data symbols, we choose the N_v -best data symbols generating the smallest MSE as virtual pilots (see Fig. 4). Although this approach does not consider the correlation among virtual pilot symbols and hence is not optimal, computational complexity is much smaller than the approach using all possible symbol combinations. Also, this approach is effective in improving the quality of channel re-estimation.

Let $\hat{\mathbf{h}}_0^{(n)}$ be the estimated channel vector when the *n*-th data symbol is used as a virtual pilot, then the MSE metric ε_n for the hypothetical selection of the n-th data symbol is expressed as

$$\varepsilon_{n} = E \left[\|\mathbf{h}_{0} - \hat{\mathbf{h}}_{0}^{(n)}\|_{2}^{2} \right] = \operatorname{tr} \left(\operatorname{Cov} \left(\mathbf{h}_{0} - \tilde{\Omega} \tilde{\Sigma}^{-1} \begin{bmatrix} \mathbf{z}_{p} \\ \mathbf{y}_{v}^{(n)} \end{bmatrix} \right) \right) \\
= \operatorname{tr} \left(\operatorname{Cov} \left(\mathbf{h}_{0} \right) - \operatorname{Cov} \left(\tilde{\Omega} \tilde{\Sigma}^{-1} \begin{bmatrix} \mathbf{y}_{p} \\ \mathbf{y}_{v}^{(n)} \end{bmatrix} \right) \right) \\
= \operatorname{tr} \left(\operatorname{Cov} \left(\mathbf{h}_{0} \right) - \tilde{\Omega} \tilde{\Sigma}^{-1} \tilde{\Omega}^{H} \right) \tag{34}$$

where

$$\tilde{\Omega} = \operatorname{Cov}\left(\mathbf{h}_{0}, \begin{bmatrix} \mathbf{y}_{p} \\ \mathbf{y}_{v}^{(n)} \end{bmatrix}\right)
= \left[E[\mathbf{h}_{0}\mathbf{y}_{p}^{H}] \ E[\mathbf{h}_{0}\mathbf{y}_{v}^{(n)H}]\right]
= \left[\mathbf{C}_{hh}\mathbf{P}_{0}^{H} \ (\bar{\mathbf{s}}_{0}^{(n)})^{*}\mathbf{C}_{hh}\right]$$
(35)

and

$$\tilde{\Sigma} = \operatorname{Cov}\left(\begin{bmatrix} \mathbf{y}_{p} \\ \mathbf{y}_{v}^{(n)} \end{bmatrix}\right)
= \begin{bmatrix} E[\mathbf{y}_{p}\mathbf{y}_{p}^{H}] & E[\mathbf{y}_{p}\mathbf{y}_{v}^{(n)H}] \\ E[\mathbf{y}_{v}^{(n)}\mathbf{y}_{p}^{H}] & E[\mathbf{y}_{v}^{(n)}\mathbf{y}_{v}^{(n)H}] \end{bmatrix}
= \begin{bmatrix} \mathbf{P}_{0}\mathbf{C}_{hh}\mathbf{P}_{0}^{H} + \eta_{p}\mathbf{I} & (\bar{s}_{0}^{(n)})^{*}\mathbf{P}_{0}\mathbf{C}_{hh} \\ (\bar{s}_{0}^{(n)})^{*}\mathbf{C}_{hh}\mathbf{P}_{0}^{H} & \bar{\lambda}_{0}^{(n)}\mathbf{C}_{hh} + \eta_{v}\mathbf{I} \end{bmatrix}$$
(36)

using $\mathbf{y}_v^{(n)} = s_0^{(n)} \mathbf{h}_0 + \mathbf{z}_v^{(n)}$ is the virtual pilot observation vector for the *n*-th data symbol. From (34), (35), and (36), ε_n is expressed as (see Appendix)

$$\varepsilon_{n} = N(1 - \gamma_{p}^{2}(1 + \gamma_{p}) \frac{\bar{\lambda}_{0}^{(n)}}{\bar{\lambda}_{0}^{(n)} + \eta_{v}} (\bar{\lambda}_{0}^{(n)})^{2}$$

$$- \gamma_{p}^{2} \left(\frac{2\eta_{v}\bar{\lambda}_{0}^{(n)} + \eta_{v}^{2}}{\bar{\lambda}_{0}^{(n)} + \eta_{v}} \right) \bar{\lambda}_{0}^{(n)} + \gamma_{p} \frac{(\bar{\lambda}_{0}^{(n)})^{3}}{(\bar{\lambda}_{0}^{(n)} + \eta_{v})^{3}}$$

$$+ \frac{(\bar{\lambda}_{0}^{(n)})^{2}}{(\bar{\lambda}_{0}^{(n)} + \eta_{v})^{2}} \frac{N_{p}^{2}}{\gamma_{p}} + \frac{\bar{\lambda}_{0}^{(n)}}{\bar{\lambda}_{0}^{(n)} + \eta_{v}} (2\gamma_{p} + N_{p}^{2} - 1) - \gamma_{p})$$
(37)

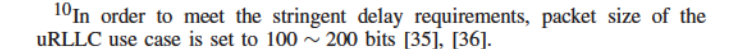
where $\gamma_p = \frac{N_p}{N_p + \eta_p}$. Note that ε_n depends on the reliability of soft decisions (i.e., the second order statistic of data symbol $\bar{\lambda}_0^{(n)}$ in (33)). Hence, in order to achieve the minimum MSE, the desired data symbol maximizing $\bar{\lambda}_0^{(n)}$ should be chosen as the virtual pilot. Once ε_n for all n are computed, we choose N_v data symbols minimizing ε_n (see Fig. 7). Observations of virtual pilots and normal pilots are used for the re-estimation of the channel vector.

V. SIMULATION RESULTS AND DISCUSSIONS

In this section, we evaluate the performance of the proposed algorithm. In our setup, we assume that adjacent interfering devices are randomly located on a square (of area $100 \ m^2$). The target receiver is located at center and the target transmit device is located 1 meter away from the receiver. The packet size is set to $100 \ \text{bits.}^{10}$ As a performance measure, we consider a packet error rate (PER). We assume that elements of channel vector for each device are i.i.d. zero mean complex Gaussian random variables with unit variance.

In our simulations, we study the performance of the following receiver techniques:

 MMSE receiver with estimated CSI (conventional MMSE receiver) [15]: we set the interference training period as K.



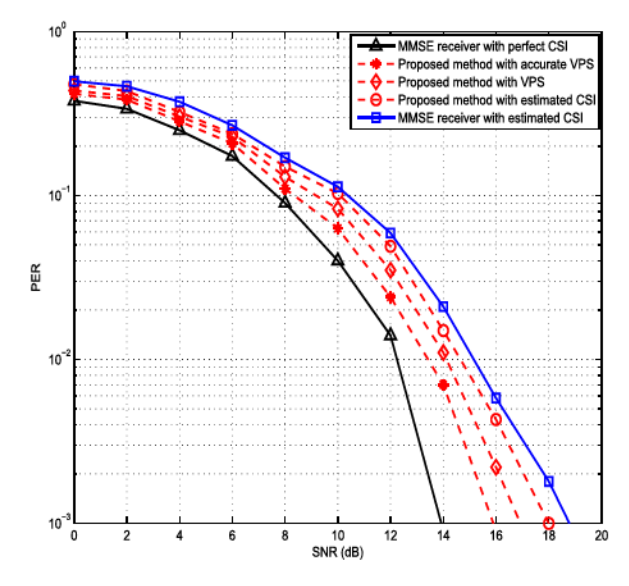


Fig. 5. PER performance of receiver techniques as a function of SNR. We set r = 1/2, N = 6, J = 6, $N_p = 10$, K = 10, $N_d = 40$, $N'_d = 50$, $N_b = 60$, $N_n = 20$.

- 2) Proposed method with estimated CSI: we set the interference training period as $N_d = N_b N_p$.
- Proposed method with virtual pilot signals (VPS): we choose N_v-best virtual pilots with the smallest MSE for the channel re-estimation.
- 4) Proposed method with accurate VPS: we use N_v -accurate data symbols as virtual pilots in the re-estimation of the channel vector.

In Fig. 5, we plot the PER performance of all techniques under consideration. In this simulations, we use the half rate $(r=\frac{1}{2})$ convolutional code with feedback polynomial $1+D+D^2$ and feedforward polynomial $1+D^2$.¹¹ In the proposed method, 20 data symbols are used as VPS $(N_v=20)$. We set J=6 as dominant neighboring interfering devices. We observe that the proposed method with VPS achieves more than 2 dB gain over the conventional MMSE receiver at 10^{-3} PER point. We also observe that the addition of VPS achieves more than 1 dB gain over the proposed method without VPS.

In Fig. 6, we plot the PER performance with code rate $r = \frac{3}{4}$ convolutional code with feedback polynomial $1 + D^2 + D^3$ and feedforward polynomial $1 + D + D^3$. We observe from the figure that the performance gain of the proposed method with VPS is 2 dB over the conventional MMSE receiver and more than 0.8 dB over the proposed method without VPS at 10^{-3} PER point.

In Fig. 8, we plot the PER performance result of the schemes we considered with polar code and convolutional codes. We set the block length N_b as 64 since the block length of the polar code should be always a power of 2. We observe from the figure that the proposed method with polar code is superior to the convolutional code based schemes. Specifically, we observe that use of polar code will bring one dB over the convolutional code at 10^{-3} PER point.

¹¹In IoT systems, convolutional codes are preferred over turbo or LDPC codes [5].

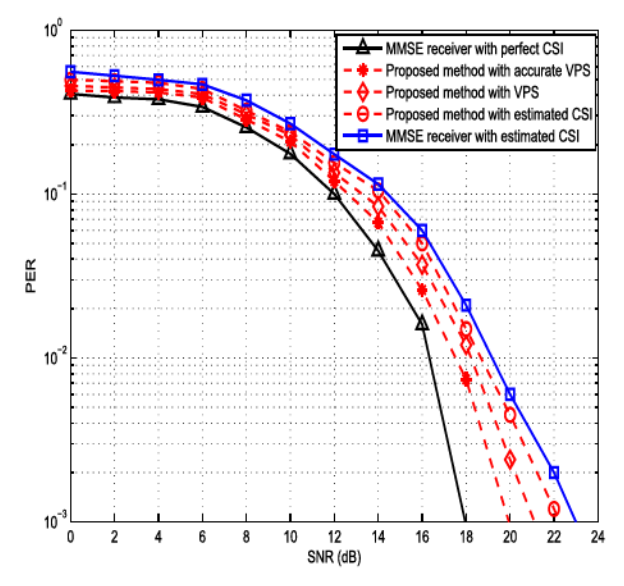


Fig. 6. PER performance of receiver techniques as a function of SNR. We set $r=3/4,\ N=6,\ J=6,\ N_p=10,\ K=10,\ N_d=40,\ N_d'=50,\ N_b=60,\ N_v=20.$

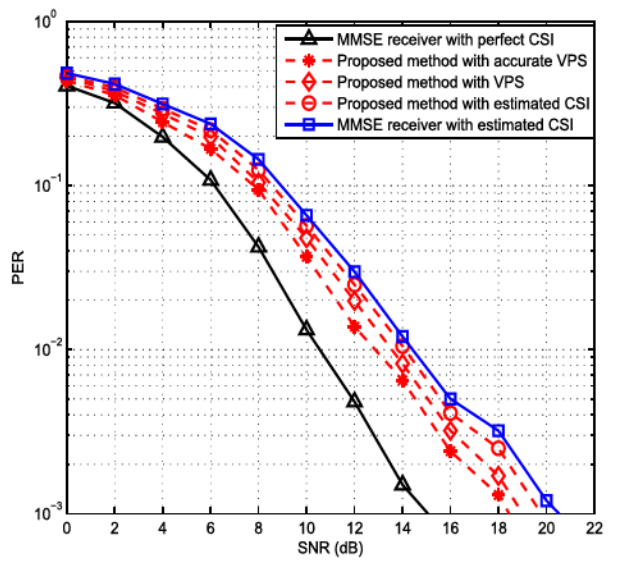


Fig. 7. PER performance of receiver techniques as a function of SNR over the Rician fading channel. We set r=1/2, N=6, J=6, $N_p=10$, K=10, $N_d=40$, $N_d'=50$, $N_b=60$, $N_v=20$.

We next consider the performance of the proposed method over the Rician fading channel. Note that Rician fading includes the line-of-sight (LOS) signal propagation, which can be more general and realistic than Rayleigh fading [33]. In this simulations, we use the Rician K-factor K=6 dB. Due to the LOS components of the interference channels, we observe from Fig. 7 that the performance of all receivers under consideration is worse than the case using the Rayleigh fading channel. From numerical results, the proposed method with VPS is still effective and achieving more than 1.5 dB gain over the conventional MMSE receiver at 10^{-3} PER point. We also observe that the addition of VPS achieves around 0.8 dB gain over the proposed method without VPS.

In Fig. 9, we plot the throughput as a function of the number of receive antennas N for temporally correlated channels.

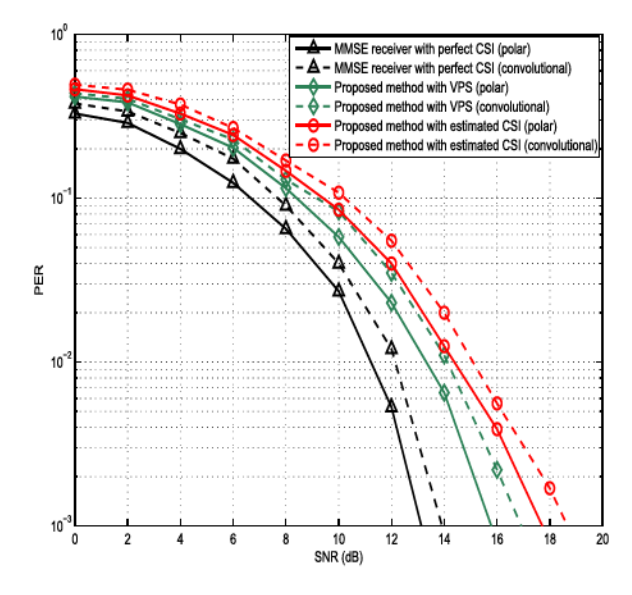


Fig. 8. PER performance of receiver techniques as a function of SNR with polar code and convolutional codes. We set r = 1/2, N = 6, J = 6, $N_p = 10$, $N'_d = 54$, $N_b = 64$, $N_v = 20$.

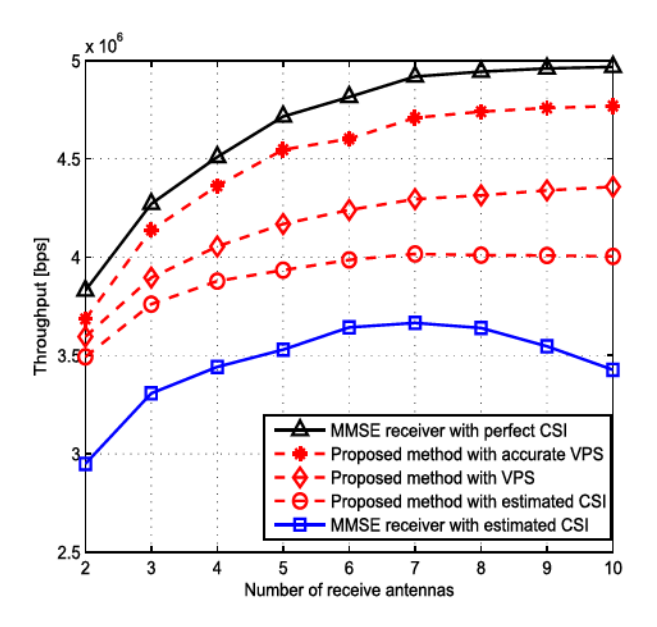


Fig. 9. Throughput of receiver techniques as a function of number of receive antennas N for temporally-correlated block fading channel. We set SNR = 0 dB, $r = \frac{1}{2}$, J = 6, $N_p = 10$, K = 10, $N_d = 40$, $N_d' = 50$, $N_b = 60$, $N_v = 20$.

We consider temporally correlated channels that are modeled by a first order Gauss-Markov process [34] as $\mathbf{h}[k] = \xi \mathbf{h}[k-1] + \sqrt{1-\xi^2}\mathbf{g}[k]$ where $\mathbf{g}[k]$ is the innovation process, which is modeled as having i.i.d entries distributed with $\mathcal{CN}(0,1)$ and $0 \le \xi \le 1$ is the temporal correlation coefficient. In this simulations, we use $\xi = 0.9881$ for the moderate mobile speed. To evaluate the throughput, we present Monte-Carlo simulation results with 10000 iterations. Since each iteration consists of 10 fading blocks, the maximum throughput is about 5 Mbps. As observed in (7) and (15), when the number of receive antennas N increases, the training period used for the sample covariance matrix computation

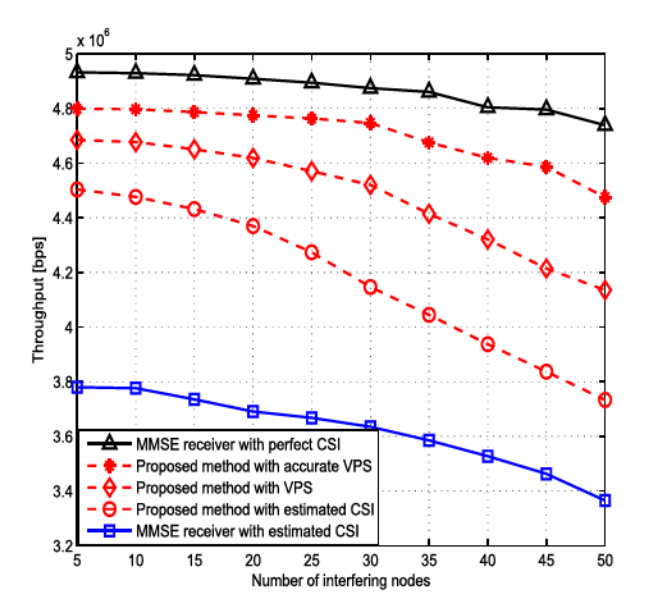
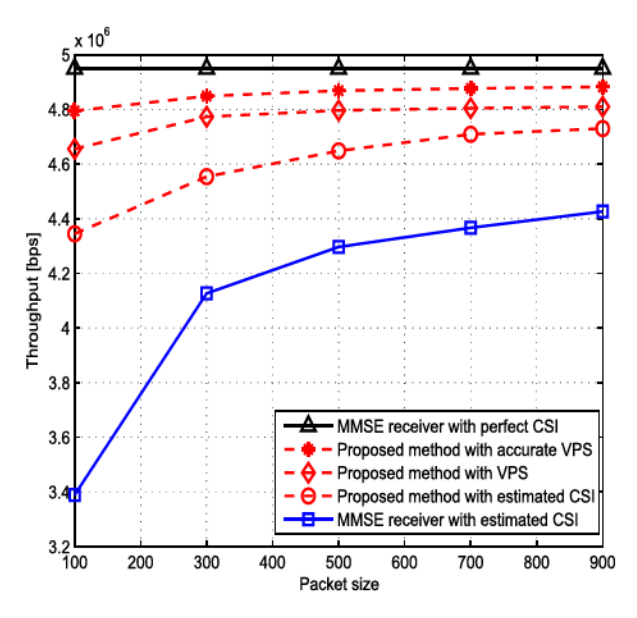


Fig. 10. Throughput of receiver techniques as a function of interfering devices for temporally-correlated block fading channel. We set SNR = 10 dB, $r = \frac{1}{2}$, N = 6, $N_p = 10$, K = 10, $N_d = 40$, $N_d' = 50$, $N_b = 60$, $N_v = 20$.



Throughput of receiver techniques as a function of N_b for temporally-correlated block fading channel. We set J=6, SNR = 0 dB, N = 8, $N_p = 0.1N_b$, $K = 0.1N_b$, $N_d = 0.8N_b$, $N'_d = 0.9N_b$, $N_v = 0.2N_d$.

should also be increased to attain the target SINR. Thus, when the interfering training period K is fixed, the scaling factor $\left(1 - \frac{N-1}{K+1}\right)$ decreases with the number of receiver antennas N. As a result, we observe the throughput degradation on the conventional MMSE receiver when number of receive antennas is large (N > 7). Whereas, the throughput of the proposed VPS scheme increases with the number of receive antennas N.

In Fig. 10, we plot the throughput as a function of the number of adjacent interfering devices J. Since the accuracy of the covariance matrix estimation deteriorates as the number of interfering devices J grows large, we see that the throughput decreases with J for all methods simulated. We observe that the proposed method using VPS performs close to the MMSE receiver using the perfect CSI (5 \sim 7% throughput loss) and also provides 21% gain over the conventional MMSE receiver when $J \leq 30$.

Finally, in Fig. 11, we show the throughput as a function of packet size N_b . We observe that the rate loss of the proposed method over the MMSE receiver with perfect CSI is around $6\% \sim 13\%$, which is far better than the rate loss of the conventional MMSE receiver (12% \sim 32%). These results demonstrate that the proposed method has clear benefit over the conventional MMSE receiver in the short packet transmission.

VI. CONCLUSION

Short packet transmission systems are critical to fulfilling the stringent low latency requirements of the fifth generation (5G) wireless standards. We proposed a receiver technique suited to short packet transmission. Our work was motivated by the observation that the insufficient training period resulting from a small packet structure causes severe degradation in the desired channel and interference covariance matrix estimation. By exploiting reliable symbols in the data transmission period, the proposed receiver algorithm achieves improved estimation and eventual throughput gain. Although our study in this work focused on the low latency communication, the main concept can be readily extended to massive machine-type communications scenario (mMTC use case) and high throughput massive MIMO scenario (eMBB use case) of 5G wireless communications. In both scenarios, the channel estimation quality would be crucial to achieve the desired goal. Also a noncoherent approach that does not rely on the pilot signal might be alternative option for uRLLC communication.

APPENDIX DERIVATION OF (37)

Recall from (34) that ε_n is given by

$$\varepsilon_n = \operatorname{tr}\left(\operatorname{Cov}\left(\mathbf{h}_0\right) - \tilde{\Omega}\tilde{\boldsymbol{\Sigma}}^{-1}\tilde{\boldsymbol{\Omega}}^H\right)$$
 (38)

where

$$\tilde{\Omega} = \text{Cov}\left(\mathbf{h}_0, \begin{bmatrix} \mathbf{y}_p \\ \mathbf{v}_n^{(n)} \end{bmatrix}\right) = \begin{bmatrix} \mathbf{C}_{hh} \mathbf{P}_0^H & (\bar{s}_0^{(n)})^* \mathbf{C}_{hh} \end{bmatrix} \quad (39)$$

and

$$\tilde{\Sigma} = \operatorname{Cov}\left(\begin{bmatrix} \mathbf{y}_{p} \\ \mathbf{y}_{v}^{(n)} \end{bmatrix}, \begin{bmatrix} \mathbf{y}_{p} \\ \mathbf{y}_{v}^{(n)} \end{bmatrix}\right) \\
= \begin{bmatrix} \mathbf{P}_{0}\mathbf{C}_{hh}\mathbf{P}_{0}^{H} + \eta_{p}\mathbf{I} & \mathbf{P}_{0}\mathbf{C}_{hh}(\bar{s}_{0}^{(n)})^{*} \\ \bar{s}_{0}^{(n)}\mathbf{C}_{hh}\mathbf{P}_{0}^{H} & \bar{\lambda}_{0}^{(n)}\mathbf{C}_{hh} + \eta_{v}\mathbf{I} \end{bmatrix}.$$
(40)

For convenience, we let

$$\begin{bmatrix} \Omega_1 & \Omega_2 \end{bmatrix} = \begin{bmatrix} C_{hh} P_0^H & (\bar{s}_0^{(n)})^* C_{hh} \end{bmatrix}, \tag{41}$$

$$\begin{bmatrix} \mathbf{\Omega}_{1} & \mathbf{\Omega}_{2} \end{bmatrix} = \begin{bmatrix} \mathbf{C}_{hh} \mathbf{P}_{0}^{H} & (\bar{\mathbf{s}}_{0}^{(n)})^{*} \mathbf{C}_{hh} \end{bmatrix}, \tag{41}$$

$$\begin{bmatrix} \mathbf{\Sigma}_{11} & \mathbf{\Sigma}_{12} \\ \mathbf{\Sigma}_{21} & \mathbf{\Sigma}_{22} \end{bmatrix} = \begin{bmatrix} \mathbf{P}_{0} \mathbf{C}_{hh} \mathbf{P}_{0}^{H} + \eta_{p} \mathbf{I} & \mathbf{P}_{0} \mathbf{C}_{hh} (\bar{\mathbf{s}}_{0}^{(n)})^{*} \\ \bar{\mathbf{s}}_{0}^{(n)} \mathbf{C}_{hh} \mathbf{P}_{0}^{H} & \bar{\lambda}_{0}^{(n)} \mathbf{C}_{hh} + \eta_{v} \mathbf{I} \end{bmatrix}, \tag{42}$$

$$\begin{bmatrix} \Gamma_{11} & \Gamma_{12} \\ \Gamma_{21} & \Gamma_{22} \end{bmatrix} = \begin{bmatrix} \Sigma_{11} & \Sigma_{12} \\ \Sigma_{21} & \Sigma_{22} \end{bmatrix}^{-1}, \tag{43}$$

then

$$\varepsilon_{n} = \operatorname{tr} \left(\mathbf{C}_{hh} - \begin{bmatrix} \mathbf{\Omega}_{1} & \mathbf{\Omega}_{2} \end{bmatrix} \begin{bmatrix} \mathbf{\Gamma}_{11} & \mathbf{\Gamma}_{12} \\ \mathbf{\Gamma}_{21} & \mathbf{\Gamma}_{22} \end{bmatrix} \begin{bmatrix} \mathbf{\Omega}_{1} & \mathbf{\Omega}_{2} \end{bmatrix}^{H} \right)
= \operatorname{tr} (\mathbf{C}_{hh} - \mathbf{\Omega}_{1} \mathbf{\Gamma}_{11} \mathbf{\Omega}_{1}^{H} - \mathbf{\Omega}_{2} \mathbf{\Gamma}_{21} \mathbf{\Omega}_{1}^{H}
- \mathbf{\Omega}_{1} \mathbf{\Gamma}_{12} \mathbf{\Omega}_{2}^{H} - \mathbf{\Omega}_{2} \mathbf{\Gamma}_{22} \mathbf{\Omega}_{2}^{H} \right).$$
(44)

Using the inversion formula of partitioned matrices [20], we have

$$\begin{split} &\Gamma_{11} = (\Sigma_{11} - \Sigma_{12} \Sigma_{22}^{-1} \Sigma_{21})^{-1} \\ &\Gamma_{12} = -\Sigma_{11}^{-1} \Sigma_{12} (\Sigma_{22} - \Sigma_{21} \Sigma_{11}^{-1} \Sigma_{21})^{-1} \\ &\Gamma_{21} = -\Sigma_{22}^{-1} \Sigma_{21} (\Sigma_{11} - \Sigma_{12} \Sigma_{22}^{-1} \Sigma_{21})^{-1} \\ &\Gamma_{22} = (\Sigma_{22} - \Sigma_{21} \Sigma_{11}^{-1} \Sigma_{12})^{-1}. \end{split} \tag{45}$$

Using (45), we further have

$$\Omega_{1}\Gamma_{11}\Omega_{1}^{H} = C_{hh}P_{0}^{H}\Gamma_{11}P_{0}C_{hh}
\Omega_{2}\Gamma_{21}\Omega_{1}^{H} = (\bar{s}_{0}^{(n)})^{*}C_{hh}\Gamma_{21}P_{0}C_{hh}
\Omega_{1}\Gamma_{12}\Omega_{2}^{H} = \bar{s}_{0}^{(n)}C_{hh}P_{0}^{H}\Gamma_{12}C_{hh}
\Omega_{2}\Gamma_{22}\Omega_{2}^{H} = \bar{\lambda}_{0}^{(n)}C_{hh}\Gamma_{22}C_{hh}.$$
(46)

Using the matrix inversion lemma $((A - BD^{-1}C)^{-1} = A^{-1} + A^{-1}B(D - CA^{-1}B)CA^{-1})$ and noting that

$$\Phi = \mathbf{P}_{0}^{H} \mathbf{\Sigma}_{11} \mathbf{P}_{0}
\Phi' = \mathbf{P}_{0}^{H} \mathbf{\Sigma}_{11}^{-1} \mathbf{P}_{0}
\Psi = \bar{\lambda}_{0}^{(n)} \mathbf{\Sigma}_{22}
\Psi' = \bar{\lambda}_{0}^{(n)} \mathbf{\Sigma}_{22}^{-1},$$
(47)

we further have

$$\begin{split} \Omega_{1}\Gamma_{11}\Omega_{1}^{H} &= C_{hh}\Phi'(I + C_{hh}\Psi C_{hh}\Phi' - (\bar{\lambda}_{0}^{(n)})^{2}C_{hh} \\ &\times \Phi'C_{hh}C_{hh}\Phi')C_{hh} \\ \Omega_{2}\Gamma_{21}\Omega_{1}^{H} &= -C_{hh}\Psi'C_{hh}(I + \Phi'C_{hh}\Psi C_{hh} - (\bar{\lambda}_{0}^{(n)})^{2}\Phi'C_{hh} \\ &\times C_{hh}\Phi'C_{hh}C_{hh})\Phi'C_{hh} \\ \Omega_{1}\Gamma_{12}\Omega_{2}^{H} &= -C_{hh}\Phi'C_{hh}(I + \Psi'C_{hh}\Phi C_{hh} - \Psi' \\ &\times C_{hh}^{2}\Psi'C_{hh}^{2})\Psi'C_{hh} \\ \Omega_{2}\Gamma_{22}\Omega_{2}^{H} &= C_{hh}\Psi'(I + C_{hh}\Phi C_{hh}\Psi' - C_{hh}^{2}\Psi'C_{hh}^{2}\Psi')C_{hh}. \end{split}$$

$$(48)$$

Under the assumption that there is no correlation among receive antennas, $C_{hh} = I$, and hence (47) becomes

$$\Phi = \mathbf{P}_{0}^{H}(\mathbf{P}_{0}\mathbf{P}_{0}^{H} + \eta_{p}\mathbf{I})\mathbf{P}_{0} = N_{p}(N_{p} + \eta_{p})\mathbf{I}$$

$$\Phi' = \mathbf{P}_{0}^{H}(\mathbf{P}_{0}\mathbf{P}_{0}^{H} + \eta_{p}\mathbf{I})^{-1}\mathbf{P}_{0} = \frac{N_{p}}{N_{p} + \eta_{p}}\mathbf{I}$$

$$\Psi = (\bar{s}_{0}^{(n)})^{*}\mathbf{I}(\bar{\lambda}_{0}^{(n)}\mathbf{I} + \eta_{v}\mathbf{I})\bar{s}_{0}^{(n)}\mathbf{I} = \bar{\lambda}_{0}^{(n)}(\bar{\lambda}_{0}^{(n)} + \eta_{v})\mathbf{I}$$

$$\Psi' = (\bar{s}_{0}^{(n)})^{*}\mathbf{I}(\bar{\lambda}_{0}^{(n)}\mathbf{I} + \eta_{v}\mathbf{I})^{-1}\bar{s}_{0}^{(n)}\mathbf{I} = \frac{\bar{\lambda}_{0}^{(n)}}{\bar{\lambda}_{0}^{(n)} + \eta_{v}}\mathbf{I}.$$
(49)

Plugging (48) and (49) into (44) and after some manipulations, we have

$$\varepsilon_n = \text{tr}(\mathbf{I} - ((\Phi')^2 \Psi' + (\Phi')^2) \Psi - (\bar{\lambda}_0^{(n)})^2 ((\Phi')^3 \Psi' + (\Phi')^2) + (\mathbf{I} - \Phi') (\Psi')^3 + \Phi(\Psi')^2 - (\mathbf{I} - \Phi' \Phi - 2\Phi') \Psi' - \Phi')$$

$$= N(1 - \gamma_p^2 (1 + \gamma_p) \frac{\bar{\lambda}_0^{(n)}}{\bar{\lambda}_0^{(n)} + \eta_v} (\bar{\lambda}_0^{(n)})^2 - \gamma_p^2 (\frac{2\eta_v \bar{\lambda}_0^{(n)} + \eta_v^2}{\bar{\lambda}_0^{(n)} + \eta_v})$$

$$\times \bar{\lambda}_0^{(n)} + \gamma_p \frac{(\bar{\lambda}_0^{(n)})^3}{(\bar{\lambda}_0^{(n)} + \eta_v)^3} + \frac{(\bar{\lambda}_0^{(n)})^2}{(\bar{\lambda}_0^{(n)} + \eta_v)^2} \frac{N_p^2}{\gamma_p}$$

$$+ \frac{\bar{\lambda}_0^{(n)}}{\bar{\lambda}_0^{(n)} + \eta_v} (2\gamma_p + N_p^2 - 1) - \gamma_p)$$
(50)

where $\gamma_p = \frac{N_p}{N_p + \eta_p}$.

REFERENCES

- B. Lee, S. Park, D. J. Love, H. Ji, and B. Shim, "Packet structure and receiver design for low-latency communications with ultra-small packets," in *Proc. IEEE Global Commun. (GLOBECOM) Conf.*, Dec. 2016, pp. 1–6.
- [2] L. Atzori, A. Iera, and G. Morabito, "The Internet of Things: A survey," Comput. Netw., vol. 54, no. 15, pp. 2787–2805, Oct. 2010.
- [3] E. Lähetkangas et al., "Achieving low latency and energy consumption by 5G TDD mode optimization," in Proc. IEEE Int. Conf. Commun. (ICC), Jun. 2014, pp. 1–6.
- [4] H. Ji, S. Park, J, Yeo, Y. Kim, J. Lee, and B. Shim, "Ultra reliable and low latency communications in 5G: Physical layer aspects," *IEEE Wireless Commun.*, submitted for publication.
- [5] N. Johansson, Y. P. E. Wang, E. Eriksson, and M. Hessler, "Radio access for ultra-reliable and low-latency 5G communications," in *Proc. IEEE Int. Conf. Commun. (ICC)*, Jun. 2015, pp. 1184–1189.
- [6] F. Boccardi, R. W. Heath, Jr., A. Lozano, T. L. Marzetta, and P. Popovski, "Five disruptive technology directions for 5G," *IEEE Commun. Mag.*, vol. 52, no. 2, pp. 74–80, Feb. 2014.
- [7] A. Osseiran et al., "Scenarios for 5G mobile and wireless communications: The vision of the METIS project," *IEEE Commun. Mag.*, vol. 52, no. 5, pp. 26–35, May 2014.
- [8] Y. Polyanskiy, H. V. Poor, and S. Verdú, "Channel coding rate in the finite blocklength regime," *IEEE Trans. Inf. Theory*, vol. 56, no. 5, pp. 2307–2359, May 2010.
- [9] W. Yang, G. Durisi, T. Koch, and Y. Polyanskiy, "Quasi-static multipleantenna fading channels at finite blocklength," *IEEE Trans. Inf. Theory*, vol. 60, no. 7, pp. 4232–4265, Jun. 2014.
- [10] G. Durisi, T. Koch, J. Östman, Y. Polyanskiy, and W. Yang, "Short-packet communications over multiple-antenna Rayleigh-fading channels," *IEEE Trans. Commun.*, vol. 64, no. 2, pp. 618–629, Feb. 2016.
- [11] G. Durisi, T. Koch, and P. Popovski, "Toward massive, ultrareliable, and low-latency wireless communication with short packets," *Proc. IEEE*, vol. 104, no. 9, pp. 1711–1726, Sep. 2016.
- [12] B. Makki, T. Svensson, and M. Zorzi, "Finite block-length analysis of spectrum sharing networks using rate adaptation," *IEEE Trans. Commun.*, vol. 63, no. 8, pp. 2823–2835, Aug. 2015.
- [13] B. Makki, T. Svensson, and M. Zorzi, "Wireless energy and information transmission using feedback: Infinite and finite block-length analysis," *IEEE Trans. Commun.*, vol. 64, no. 12, pp. 5304–5318, Dec. 2016.
- [14] J. Andrews, W. Choi, and R. W. Heath, Jr., "Overcoming interference in spatial multiplexing MIMO cellular networks," *IEEE Wireless Commun.*, vol. 14, no. 6, pp. 95–104, Dec. 2007.
- [15] N. Jindal, J. G. Andrews, and S. Weber, "Multi-antenna communication in ad hoc networks: Achieving MIMO gains with SIMO transmission," *IEEE Trans. Commun.*, vol. 59, no. 2, pp. 529–540, Feb. 2011.
- [16] J. Gao and H. Liu, "Decision-directed estimation of MIMO time-varying Rayleigh fading channels," *IEEE Trans. Wireless Commun.*, vol. 4, no. 4, pp. 1412–1417, Jul. 2005.
- [17] D. Yoon and J. Moon, "Soft-decision-driven channel estimation for pipelined turbo receivers," *IEEE Trans. Commun.*, vol. 59, no. 8, pp. 2141–2151, Aug. 2011.
- [18] S. Park, B. Shim, and J. Choi, "Iterative channel estimation using virtual pilot signals for MIMO-OFDM systems," *IEEE Trans. Signal Process.*, vol. 63, no. 12, pp. 3032–3045, Jun. 2015.
- [19] H. V. Poor and S. Verdú, "Probability of error in MMSE multiuser detection," *IEEE Trans. Inf. Theory*, vol. 43, no. 3, pp. 858–871, May 1997.
- [20] S. M. Kay, Fundamentals of Statistical Signal Processing: Estimation Theory. EngleWood Cliffs, NJ, USA: Prentice-Hall, 1998.

- [21] H. Gao, P. J. Smith, and M. V. Clark, "Theoretical reliability of MMSE linear diversity combining in Rayleigh-fading additive interference channels," *IEEE Trans. Commun.*, vol. 46, no. 5, pp. 666–672, May 1998.
- [22] D. Tse and P. Viswanath, Fundamentals of Wireless Communications. Cambridge, U.K.: Cambridge Univ. Press, 2005.
- [23] P. Li, D. Paul, R. Narasimhan, and J. Cioffi, "On the distribution of SINR for the MMSE MIMO receiver and performance analysis," *IEEE Trans. Inf. Theory*, vol. 52, no. 1, pp. 271–286, Jan. 2006.
- [24] N. Kim, Y. Lee, and H. Park, "Performance analysis of MIMO system with linear MMSE receiver," *IEEE Trans. Wireless Commun.*, vol. 7, no. 11, pp. 4474–4478, Nov. 2008.
- [25] J. Park, B. Lee, and B. Shim, "A MMSE vector precoding with block diagonalization for multiuser MIMO downlink," *IEEE Trans. Commun.*, vol. 60, no. 2, pp. 569–577, Feb. 2012.
- [26] S. A. M. Ghanem. (Nov. 2014). "Multiple access Gaussian channels with arbitrary inputs: Optimal precoding and power allocation." [Online]. Available: https://arxiv.org/abs/1411.0446
- [27] S. T. Veetil, K. Kuchi, and R. K. Ganti, "Performance of PZF and MMSE receivers in cellular networks with multi-user spatial multiplexing," *IEEE Trans. Wireless Commun.*, vol. 14, no. 9, pp. 4867–4878, Sep. 2015.
- [28] H. Cox, R. Zeskind, and M. Owen, "Robust adaptive beamforming," IEEE Trans. Acoust., Speech, Signal Process., vol. ASSP-35, no. 10, pp. 1365–1375, Oct. 1987.
- [29] I. Reed, J. Mallet, and L. Brennan, "Rapid convergence rate in adaptive arrays," *IEEE Trans. Aerosp. Electron. Syst.*, vol. AES-10, no. 6, pp. 853–863, Nov. 1974.
- [30] N. Goodman, "Statistical analysis based on a certain multivariate complex gaussian distribution," *Ann. Math. Stat.*, vol. 34, no. 1, pp. 152–177, Mar. 1963.
- [31] G. Fordor, P. D. Marco, and M. Telek, "On the impact of antenna correlation on the pilot-data balance in multiple antenna systems," in *Proc. IEEE Int. Conf. Commun. (ICC)*, Jun. 2015, pp. 2590–2596.
- [32] B. M. Hochwald and S. ten Brink, "Achieving near-capacity on a multiple-antenna channel," *IEEE Trans. Commun.*, vol. 51, no. 3, pp. 389–399, Mar. 2003.
- [33] J. Zhang, L. Dai, Z. He, S. Jin, and X. Li. (Mar. 2017). "Performance analysis of mixed-ADC massive MIMO systems over Rician fading channels." [Online]. Available: https://arxiv.org/abs/1703.03642
- [34] W. C. Jakes, Microwave Mobile Communications. New York, NY, USA: Wiley, 1975.
- [35] F. Fettweis and S. Alamouti, "5G: Personal mobile Internet beyond what cellular did to telephony," *IEEE Commun. Mag.*, vol. 52, no. 2, pp. 140–145, Feb. 2014.
 [36] C. Bockelmann *et al.*, "Massive machine-type communications in 5G:
- [36] C. Bockelmann et al., "Massive machine-type communications in 5G: Physical and MAC-layer solutions," *IEEE Commun. Mag.*, vol. 54, no. 9, pp. 59–65, Sep. 2016.



Byungju Lee (M'15) received the B.S. and Ph.D. degrees from the School of Information and Communication, Korea University, Seoul, South Korea, in 2008 and 2014, respectively. From 2014 to 2015, he was a Post-Doctoral Fellow with the Department of Electrical and Computer Engineering, Seoul National University. He was a Post-Doctoral Scholar with the School of Electrical and Computer Engineering, Purdue University, West Lafayette, IN, USA, from 2015 to 2017. He joined Samsung Electronics in 2017, has been involved in research and

standardization for 3GPP 5G NR. His research interests include physical layer system design for 5G wireless communications.



Sunho Park (M'16) received the B.S., M.S., and Ph.D. degrees from the School of Information and Communication, Korea University, Seoul, in 2008, 2010, and 2015, respectively. Since 2015, he has been with the Institute of New Media and Communications, Seoul National University, Seoul, South Korea, as a Research Assistant Professor. His research interests include wireless communications and signal processing.



David J. Love (S'98–M'05–SM'09–F'15) received the B.S. (Hons.), M.S.E., and Ph.D. degrees in electrical engineering from The University of Texas at Austin in 2000, 2002, and 2004, respectively. From 2000 to 2002, he was with Texas Instruments, Dallas, TX, USA. Since 2004, he has been with the School of Electrical and Computer Engineering, Purdue University, West Lafayette, IN, USA, where he is currently a Professor and recognized as a University Faculty Scholar. He leads the College of Engineering Preeminent Team on Efficient Spectrum

Usage. He has been very involved in commercialization of his research with around 30 U.S. patent filings, 27 of which have issued. He is a frequent consultant on cellular and WiFi systems, including patent licensing and litigation. His research interests are in the design and analysis of communication systems and MIMO array processing. He has served as an Editor of the IEEE Transactions on Communications, an Associate Editor of the IEEE Transactions on Signal Processing, and a Guest Editor for special issues of the IEEE Journal on Selected Areas in Communications and Networking.

Dr. Love has been recognized as the Thomson Reuters Highly Cited Researcher. He is a fellow of the Royal Statistical Society, and he has been inducted into Tau Beta Pi and Eta Kappa Nu. Along with his co-authors, he received best paper awards from the IEEE Communications Society (2016 IEEE Communications Society Stephen O. Rice Prize), the IEEE Signal Processing Society (2015 IEEE Signal Processing Society Best Paper Award), and the IEEE Vehicular Technology Society (2009 IEEE Transactions on Vehicular Technology Jack Neubauer Memorial Award). He has received multiple IEEE Global Communications Conference (Globecom) best paper awards. He was a recipient of the Fall 2010 Purdue HKN Outstanding Teacher Award, the Fall 2013 Purdue ECE Graduate Student Association Outstanding Faculty Award, and the Spring 2015 Purdue HKN Outstanding Professor Award. He was an invited participant to the 2011 NAE Frontiers of Engineering Education Symposium and the 2016 EU-US NAE Frontiers of Engineering Symposium. In 2003, he received the IEEE Vehicular Technology Society Daniel Noble Fellowship.



Hyoungju Ji (M'17) is currently pursuing the Ph.D. degree with the School of Electrical and Computer Engineering, Seoul National University, Seoul, South Korea. He joined Samsung Electronics in 2007, and has been involved in 3GPP RAN1 LTE, LTE-Adv, and LTE-A Pro technology developments and standardization. His current interests include ultra-reliable low-latency transmission, multi-antenna techniques (FD-MIMO), massive machine type communications, and IoT communications.



Byonghyo Shim (S'95–M'97–SM'09) received the B.S. and M.S. degrees in control and instrumentation engineering from Seoul National University, South Korea, in 1995 and 1997, respectively, and the M.S. degree in mathematics and the Ph.D. degree in electrical and computer engineering from the University of Illinois at Urbana–Champaign, USA, in 2004 and 2005, respectively. From 1997 and 2000, he was with the Department of Electronics Engineering, Korean Air Force Academy, as an Officer (First Lieutenant) and an Academic Full-time Instructor. From 2005 to

2007, he was with Qualcomm Inc., San Diego, CA, USA, as a Staff Engineer. From 2007 to 2014, he was with the School of Information and Communication, Korea University, Seoul, as an Associate Professor. Since 2014, he has been with the Seoul National University, where he is currently a Professor with the Department of Electrical and Computer Engineering. His research interests include wireless communications, statistical signal processing, estimation and detection, compressed sensing, and information theory.

Dr. Shim is an elected member of the Signal Processing for Communications and Networking Technical Committee of the IEEE Signal Processing Society. He was a recipient of the M. E. Van Valkenburg Research Award from the ECE Department of the University of Illinois in 2005, the Hadong Young Engineer Award from IEIE in 2010, and the Irwin Jacobs Award from Qualcomm and KICS in 2016. He has been an Associate Editor of the IEEE TRANSACTIONS ON SIGNAL PROCESSING, the IEEE WIRELESS COMMUNICATIONS LETTERS, and *Journal of Communications and Networks*, and a Guest Editor of the IEEE JOURNAL ON SELECTED AREAS IN COMMUNICATIONS.